JOURNAL OF SOLID STATE CHEMISTRY 103, 263–268 (1993)

BRIEF COMMUNICATIONS

A Transmission Electron Microscope Study of SrO-Doped $CaTiO_3$

MIRAN ČEH* AND VIKTOR KRAŠEVEC

J. Stefan Institute, University of Ljubljana, Ljubljana, Slovenia

AND DRAGO KOLAR

Department of Chemistry and Chemical Technology, University of Ljubljana, Ljubljana, Slovenia

Received April 1, 1992; in revised form July 13, 1992; accepted July 15, 1992

The microstructure of SrO-doped $CaTiO_3$ ceramics was investigated using transmission electron microscopy (TEM). It was found that the excess SrO forms insertion planar precipitates which are coherently intergrown with the $CaTiO_3$ crystal. Two different types of SrO intergrowth were observed: (101)/(001)SrO/(020) and (020)/(001)SrO/(020). The phenomenon is similar to that observed by Ruddlesden and Popper in the system $SrTiO_3$–SrO.

Introduction

Polycrystalline titanates are widely used as capacitors and materials which exhibit a positive temperature coefficient of resistivity (PTCR). The basic compounds such as $BaTiO_3$ and $SrTiO_3$ are usually modified by formation of solid solutions with other oxides and double oxides, particularly alkaline earth titanates, stannates, and zirconates. In these materials, the development of microstructure is greatly affected by nonstoichiometry. Since electrical properties depend on microstructure, it is desirable to understand the correlations between the evolution of the microstructure and the nonstoichiometry in order to control the desired electrical properties. It is known that in some ternary oxides the nonstoichiometry can be taken up by coherent intergrowth of lamellae of various homologous oxides (*1*). Tilley (*2*) reported that for SrO-excess $SrTiO_3$, the nonstoichiometry is compensated for by coherent intergrowth between the perovskite layers of $SrTiO_3$ and the layers of SrO (Ruddlesden–Popper type faults) (*3*). Fujimoto *et al.* (*4*) studied nonstoichiometric compositions $(Sr_{0.85}Ca_{0.15}O)_{1.02}TiO_2$. Again it was found that the (Sr, Ca)O-excess forms insertion planar faults of NaCl type.

The present work was undertaken in order to determine the mode of incorporation of excess SrO in $CaTiO_3$ with respect to the different lattice constants of $CaTiO_3$ compared with those of $SrTiO_3$.

Experimental

Analytical-grade starting materials were used for preparation of samples. $CaTiO_3$

* To whom correspondence should be addressed.

0022-4596/93 $5.00

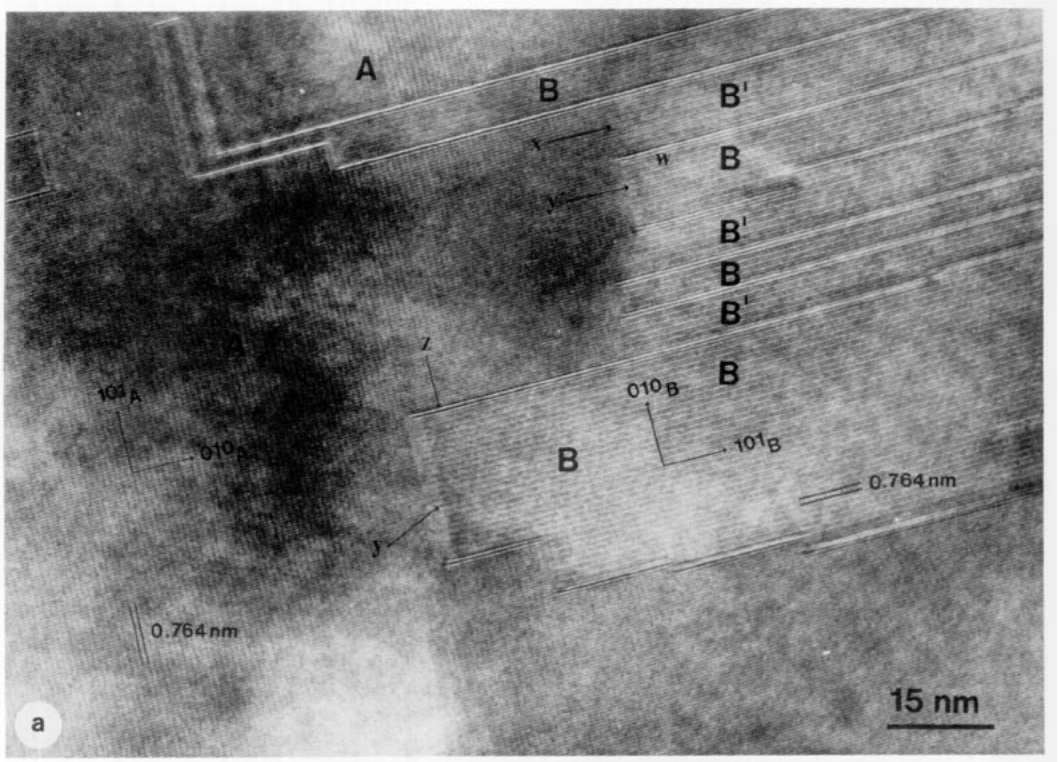
A
B
B'
x
w
y
B'
B
B'
z
B
A
$10\bar{1}_A$
010_B
010_A
$10\bar{1}_B$
B
0.764 nm
y
0.764 nm
15 nm
a

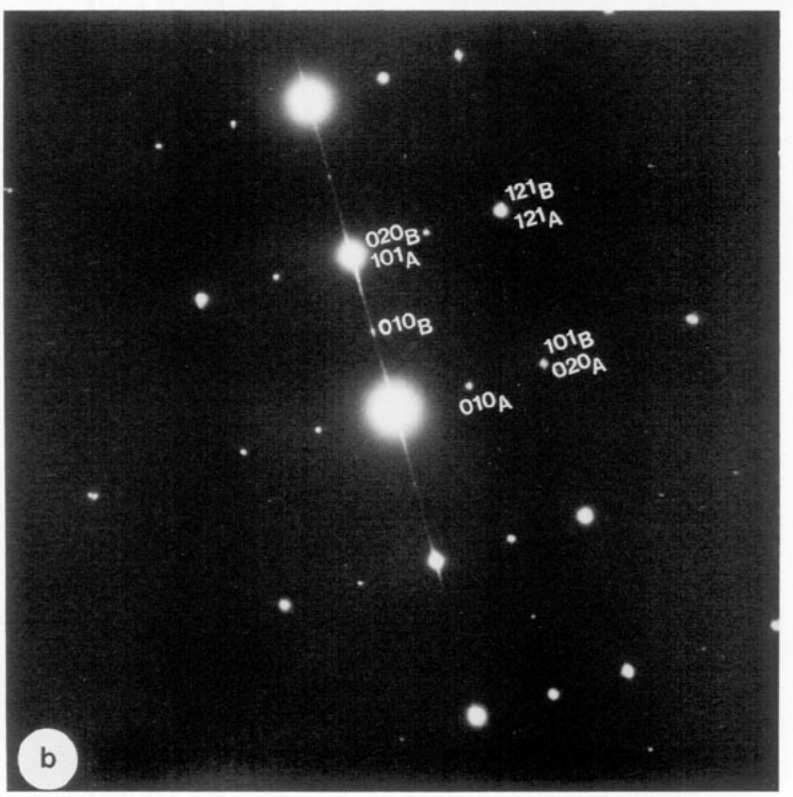
121_B
$12\bar{1}_A$
020_B
$10\bar{1}_A$
010_B
$10\bar{1}_B$
020_A
010_A
b

powders with 2 to 10 mol% SrO added were prepared by conventional ceramic procedures. SrO was added as $SrCO_3$. The mixtures of $CaTiO_3$ and $SrCO_3$ were mixed, pressed into pellets, and sintered at 1350°C for several hours. The process of calcination was repeated several times in order to obtain a higher degree of homogenization. For TEM observation the pellets were ground to concave-shaped specimens which were subsequently thinned to perforation using argon ions at 3.8 kV. Specimens were examined in a JEOL 2000 FX transmission electron microscope operating at 200 kV.

Results and Discussion

Figure 1a, which represents the lattice image of a $CaTiO_3$ thin foil as seen in the ⟨101⟩ zone, shows a typical feature which was observed only in SrO-doped specimens. The whole grain consists of domains A and B, containing lattice fringes which are mutually orthogonal. From the corresponding selected area diffraction (SAD) pattern (Fig. 1b), which is in fact a superimposition of two electron diffraction patterns of the ⟨101⟩ zone rotated by 90°, it is evident that regions A and B represent two crystallographically equivalent variants. The orientational relationships between these two variants can be written as

$$\begin{aligned} (101)_A \,||\, (010)_B \\ (010)_A \,||\, (101)_B \\ [10\bar{1}]_A \,||\, [\bar{1}01]_B \end{aligned} \qquad (1)$$

The variants A and B are separated by four different types of interfaces, X, Y, Z, and W, which can be classified according to their fringe characteristics into fringe-coinciding interfaces (X, Y) and precipitate-resembling interfaces (Z, W).

Let us first consider the simplest interface, X, which shows a continuous transition of (101) lattice fringes (region A) into (010) lattice fringes (region B). This interface obviously represents a coherent joint between two crystals which are rotated by 90° with respect to each other, as shown schematically in Fig. 2a. This is possible since the mismatch between the lattice distances of the (101) and (020) planes is almost negligible (ASTM 22-153).

Another interface which can easily be explained is the precipitate-like interface W between B and B′ (Fig. 1a). The distance between the fringes indicating the interface (two bright or two dark fringes), as measured by the adjoining lattice fringes of domain A, is exactly 1.5 times the (101) lattice distance (0.574 nm). This distance is very close to the thickness of the combined layer (CL) consisting of one perovskite layer and one SrO layer with NaCl-type structure (Ruddlesden–Popper fault) (*3*), as shown schematically in Fig. 3. It should be mentioned, however, that the shift Δ between perovskite layers, caused by the intergrown SrO layer, does not correspond to the perovskite lattice vector, although it is very close to $\frac{1}{2}\,[111]_P$ (P—perovskite). On the basis of these observations, one can conclude that the precipitate-like interface W represents a layer of SrO coherently intergrown in the crystal lattice of $CaTiO_3$. Namely, SrO has a rock salt-type structure with $a = 0.516$ nm and hence the d_{110} lattice distance is very close to the d_{101} lattice distance of $CaTiO_3$. Accordingly, the (001) layer of SrO topotactically joins the (010)

FIG. 1. (a) Lattice image of $CaTiO_3$ doped with 10 mol% SrO showing (101) and (010) lattice fringes as seen in zone ⟨101⟩. Two variants, A and B, can be distinguished. Note the four different types of interfaces marked X, Y, Z, and W. (b) The corresponding SAD pattern is a superimposition of two diffraction patterns corresponding to A and B, respectively.

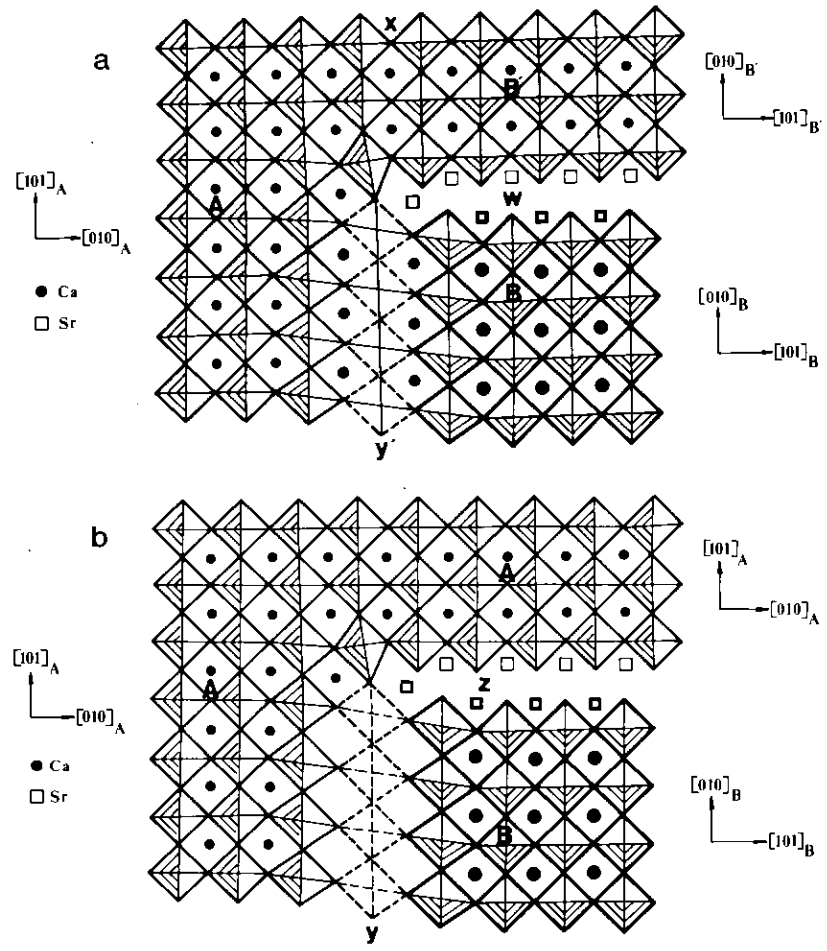

FIG. 2. (a) A schematic representation of interfaces X, W, and Y'. The interface W is a (001) layer of SrO sandwiched between $(010)_B$ and $(010)_{B'}$ layers. (b) A schematic representation of interfaces Z and Y. The interface Z is a (001) SrO layer sandwiched between $(101)_A$ and $(010)_B$ layers. Heavy-lined octahedra are raised for $\frac{1}{2}[001]_P$.

layer of $CaTiO_3$, as shown schematically in Fig. 2a. The orientational relationships between the two lattices can be written as

$$\begin{aligned}(010)_{CT} \,||\, (001)_{SrO}\\ (101)_{CT} \,||\, (110)_{SrO}\\ [\bar{1}01]_{CT} \,||\, [\bar{1}\bar{1}0]_{SrO}\end{aligned} \qquad (2)$$

The misfit between the corresponding distances of the SrO and $CaTiO_3$ lattices is given in Table I.

TABLE I

LATTICE DISTANCES OF $CaTiO_3$ AND SrO

$CaTiO_3$ ASTM Card 22-153	SrO ASTM Card 6-0520	Misfit (%)
zone $[\bar{1}01]$	zone $[\bar{1}10]$	
$d_{101} = 0.38261$	$d_{110} = 0.36487$	+4.86
$d_{\bar{1}01} = 0.38261$	$d_{\bar{1}10} = 0.36487$	+4.86
zone $[\bar{1}01]$	zone $[1\bar{1}0]$	
$d_{020} = 0.38218$	$d_{110} = 0.36487$	+4.74
$d_{\bar{1}01} = 0.38261$	$d_{1\bar{1}0} = 0.36487$	+4.86

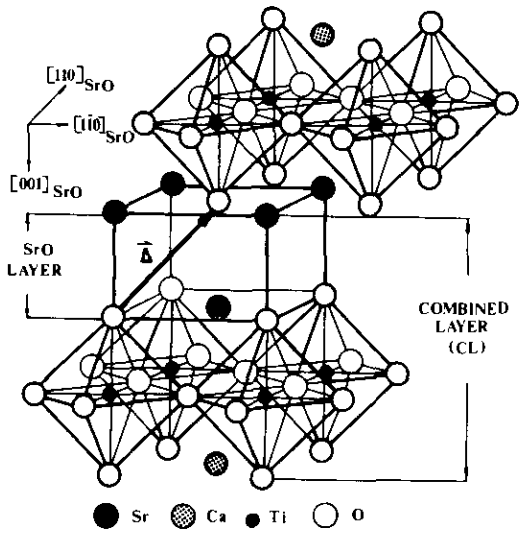

FIG. 3. A schematic representation of SrO intergrowth between perovskite layers (*3*). Note that the shift Δ is close to $\frac{1}{2}[111]_P$ of the perovskite lattice. CL is a combined layer.

The second precipitate-like interface Z is in principle equal to the interface W considered above. The only difference is the rotation of 90° around the $[\bar{1}01]$ axes. A schematic representation of the interface is given in Fig. 2b. The orientational relationships between the perovskite layer and the SrO layer for this type of interface can be written as

$$\begin{aligned}(101)_{CT} \,||\, (001)_{SrO}\\ (010)_{CT} \,||\, (110)_{SrO}\\ [\bar{1}01]_{CT} \,||\, [1\bar{1}0]_{SrO}\end{aligned} \qquad (3)$$

and the misfit between the corresponding lattice distances is evident from Table I.

From Table I it is also evident that the SrO layer is less deformed when the (001) lattice planes of SrO are parallel to the (101) lattice planes of $CaTiO_3$ and hence this configuration is energetically more favorable. The misfit of approximately 5%, however, still allows coherent intergrowth (*5*). It should be mentioned that interfaces W and Z are in principle equivalent to those found by Fujimoto *et al* (*4*).

The nature of the last type of interface between A and B (Y) is more complex. The displacement vector Δ, which is close to $\frac{1}{2}[111]_P$, brings the cations Ca and Ti on both sides of the interface Y into an antiphase position and most probably deforms the TiO_6 octahedra along the interface, as shown schematically in Fig. 2b. In this way the stoichiometry along the interface is retained. In principle one might expect a slightly different Δ between Y and Y′, since the rotation of the crystal lattice from A to B at X followed by the shift $\Delta_{B/B'}$ is not necessarily equal to the shift $\Delta_{A/B}$ followed by the rotation from B to A at Y. However, a difference in contrast which would confirm this assumption was not observed between Y and Y′. On the basis of the presented experimental evidence, the possibility that this type of interface might be nonconservative in nature could not be excluded.

In conclusion one can say that four different types of interfaces were observed in SrO-doped $CaTiO_3$ between two crystallographically orthogonal domains within a single $CaTiO_3$ grain. The precipitate-like interfaces are in fact layers of SrO which are coherently intergrown with the $CaTiO_3$ crystal lattice. SrO layers are parallel to either (101) or (020) lattice planes of $CaTiO_3$; this is possible because of the negligible difference in lattice distances between the (101) and (020) planes. The phenomenon is in principle similar to that observed by Ruddlesden and Popper (*3*) for some compounds in the system $SrTiO_3$–SrO, apart from the more sophisticated crystallographic relationships between SrO and the $CaTiO_3$ crystal lattice which are due to the different crystal structures of $CaTiO_3$ and $SrTiO_3$.

References

1. B. G. HYDE AND S. ANDERSON, "Inorganic Crystal Structures," p. 20, Wiley, New York (1989).
2. R. J. D. TILLEY, *J. Solid State Chem.* **21,** 293 (1977).
3. S. N. RUDDLESDEN AND P. POPPER, *Acta Crystallogr.* **11,** 54 (1958).
4. M. FUJIMOTO, J. TANAKA, AND S. SHIRASAKI, *Jpn. J. Appl. Phys.* **27**(7), 1162 (1988).
5. J. H. VAN DER MERWE AND C. A. B. BALL, *in* "Materials Science and Technology" (J. W. Matthews, Ed.), pp. 493–528, Academic Press, New York (1975).